Photodarkening and photobleaching of CdS microclusters grown in zeolites

1992 J. Phys.: Condens. Matter 4 5653

(http://iopscience.iop.org/0953-8984/4/26/001)

J. Phys.: Condens. Matter 4 (1992) 5653–5664. Printed in the UK

Photodarkening and photobleaching of CdS microclusters grown in zeolites

T Moyo†, K Maruyama‡ and H Endo
Department of Physics, Faculty of Science, Kyoto University, Kyoto 606-01, Japan

Received 27 January 1992

Abstract. EXAFS and photoacoustic spectroscopy have been carried out on CdS microclusters grown in Y zeolites and mordenite. Photodarkening (PD) and photobleaching (PB) are observed at low temperatures. In CdS zeolites, four new absorption bands at approximately 2, 2.3, 2.9 and 3.4 eV are induced by light with energy corresponding to the band gap at low temperatures. The optical properties appear sensitive to the annealing temperature during sample preparation. The PD and PB are discussed in terms of defect creation and annihilation.

1. Introduction

Previous reports have demonstrated the growth of II–VI semiconductor microclusters of variable size in glass [1] and zeolite [2–5] matrices. Shifts in the optical absorption edges to higher energies were observed on reduction in cluster size. This is known as the quantum size effect and is associated with the narrowing of the electronic band structure in semiconductor microclusters. It is therefore interesting to know whether II–VI semiconductor microclusters within glasses or zeolites exhibit changes in the optical properties due to light illumination and to investigate any relation with the quantum size effect.

Changes in optical properties due to illumination are well known in amorphous chalcogenide semiconductors. The behaviour is attributed to a high degree of structural flexibility and to the presence of lone-pair (LP) p electrons at the top of the valence band associated with chalcogen atoms [6]. The excitation of these LP p electrons to metastable defect states in the midgap region is responsible for the change in optical properties. Chalcogenide clusters grown inside zeolites are expected to have a high configurational freedom and their optical properties are susceptible to change under illumination. This has been shown to be true for isolated chains of Se grown in mordenite [7, 8]. Hence we have carried out investigations of the photodarkening (PD) and photobleaching (PB) of CdS microclusters grown in Y zeolite and mordenite. PD and PB are expected to yield information on the defect states created when a sample is illuminated.

Optical absorption spectra were obtained by photoacoustic spectroscopy (PAS). The results are correlated with the quantum size effect, the atomic arrangement in microclusters and the creation of metastable defect states. The annealing temperature turns out to be crucial in determining the optical properties.

† Permanent address: Physics Department, University of Zambia, PO Box 32379, Lusaka, Zambia.
‡ Present address: Graduate School of Science and Technology, Niigata University, Niigata 950-21, Japan.

0953-8984/92/265653+12$04.50

2. Experimental details

2.1. Sample preparation

Zeolites consist of corner-sharing AlO_4 and SiO_4 tetrahedra connected such that well defined pores of molecular dimensions are formed. Other metal cations can be introduced by ion exchange of the Na ions present in the original material. Hence zeolite pores can confine a wide range of molecular species. The zeolites used in the present work are synthetic Na Y zeolite ($25Na_2O \cdot 25Al_2O_3 \cdot 142SiO_2$) (TSZ320NAA) and Na mordenite ($Na_2O \cdot Al_2O_3 \cdot 20SiO_2$) (TSZ640) [7–9] supplied by the Tosoh Manufacturing Co., Ltd. Mordenite (M) consists of 6.7 Å channels and Y zeolite consists of interconnected sodalite cages (about 5 Å) and supercages (about 13 Å) [10]. It is intended that the semiconductor species grow inside the zeolite cavities. This is made possible by the good porosity and ion exchange properties of zeolites.

The Cd ions needed to replace Na ions in zeolites were derived from 99% pure cadmium nitrate crystals which were dissolved in 200 ml of distilled water. 3 g of zeolite powder were added to the solution and stirred well. The mixture was covered by Al foil and left to stand at room temperature for at least 24 h to allow for cation exchange to take place. The zeolite was filtered and washed several times to remove unexchanged Cd ions. The final filtered zeolite was dried at 80 °C for at least 5 h. The powdered sample now denoted as Cd (M or Y) zeolite was packed in an air-tight bottle and stored at room temperature. Different Cd loadings of the zeolites were obtained by varying the concentration of Cd cations in solution. The chemical composition of the samples was determined from an atomic absorption spectrochemical analysis.

We used 0.2 g of Cd (M or Y) to react with H_2S in order to produce CdS in zeolites. The zeolite was first dehydrated at about 350 °C for 3 h under a high vacuum (about 10^{-7} Torr) in a Pyrex glass tube and then brought into contact with H_2S gas which was released from a commercially available polymer medium by heating. After exposure to H_2S gas, the samples were heated at 100 °C for 1 d. The S-to-Cd ratio in the sample was determined to be about unity by x-ray fluorescence analysis.

2.2. X-ray diffraction

X-ray diffraction spectra were obtained for Na Y and Cd Y samples at room temperature and after reaction with H_2S. The spectra were used as a quick indicator of the quality of the samples produced. The position of the spectral lines hardly changed at every stage, showing that the zeolite structures were maintained. The intensities of the spectral lines reduced after cation exchange. This shows successful adsorption of the desired atoms. Furthermore, x-ray spectra were a good indicator of the different Cd loadings of our samples. The line intensities were systematically higher in samples with lower Cd loadings. For example the [110] line appears to be very sensitive to Cd loading.

Figure 1 shows the intensities of some Cd Y lines normalized with respect to Na Y lines and plotted against Cd concentration. The Cd loading appears to be saturated beyond an optimum concentration of Cd in solution. The maximum exchange fraction is about 72%.

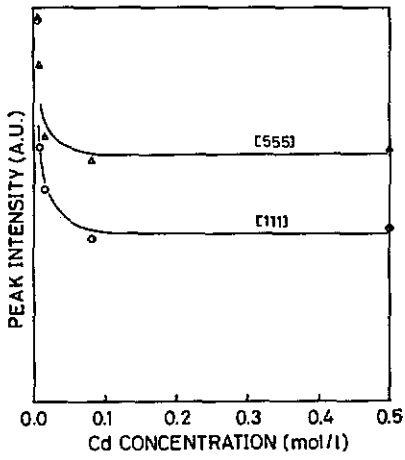

Figure 1. Cd Y powder x-ray intensities of [111] and [555] lines plotted against the Cd concentration in 200 ml solution.

2.3. EXAFS

The EXAFS experiments around the Cd K edge for Cd Y and CdS Y were carried out using the spectrometer installed at the BL-10B station of the Photon Factory in the National Laboratory for High Energy Physics [11]. With an Si(311) channel cut monochromator, an energy resolution of 1.1 eV at 9 keV was achieved with a typical photon flux of 10^9 photons s^{-1} when the storage ring was operated at 2.5 GeV and 300 mA. The zeolite sample was packed in a copper holder with Mylar windows under an He atmosphere to prevent hydration. The measurements were carried out at 80 K. The surveying energy region for the x-ray absorption spectra was from 26.4 to 27.8 keV. In a typical run it took 20 min to survey the energy region around the Cd K edge. For the Cd Y sample used in the present study, the fraction of Na cations exchanged for Cd is 72% and the CdS Y sample contains 18 wt% CdS. Further details of the experimental procedure and data analysis have been described elsewhere [8, 12].

2.4. Photoacoustic spectroscopy

The basic design and operation of the instrumentation for PAS employed here has been described elsewhere [7]. In PAS, the absorption of pulsed light causes periodic heating and cooling of the sample. This causes the He gas in the sample chamber to expand and contract periodically, creating sound waves which are detected with a microphone. By varying the wavelength of the incident light we can obtain an absorption spectrum characteristic of the sample.

The absorption spectra were obtained in the wavelength range 250–1600 nm. Sample loading was carried out in a plastic chamber filled with He gas to prevent hydration of the sample. The sample holder is attached to a cryostat which allows measurements from 300 K to liquid-He temperature. However, the present photoacoustic (PA) cell limits stable measurements to about 30 K. The sample chamber was finally replenished with fresh He gas and sealed off. During optical absorption scans at low temperatures, the probing light was dimmed by a mesh filter to minimize the PD effect produced by the light. Data acquisition was effected by remote control.

3. Results and discussion

3.1. EXAFS measurements of Cd Y and CdS Y

Figures 2(*a*) and 2(*b*) show the Cd K edge EXAFS oscillation $\chi(k)$ for Cd Y and CdS Y, respectively, as a function of photoelectron wavenumber k. The amplitude of $\chi(k)$ for Cd Y decreases rapidly with increasing k and no oscillation was observed in the high-k region beyond 10 Å^{-1}. The amplitude of $\chi(k)$ is proportional to the backward-scattering amplitude of electrons from the neighbouring atoms around the Cd atom. Such a rapid reduction in the $\chi(k)$ amplitude in the high-k region is typical of a spectrum for light atoms such as O or Si. This implies that the Cd atom bonds to O or Si atoms. It is noted that the EXAFS spectrum for CdS Y is substantially different from that for Cd Y.

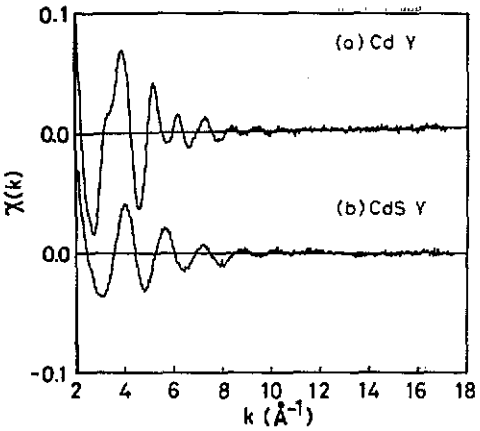

Figure 2. The EXAFS oscillation $\chi(k)$ near the Cd K edge for (*a*) Cd Y and (*b*) CdS Y.

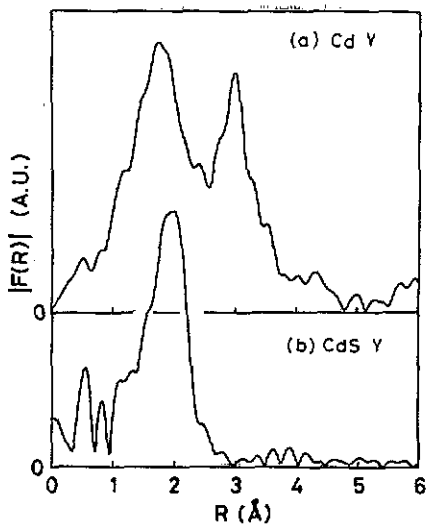

Figure 3. The radial distribution function $|F(r)|$ around the Cd atom for (*a*) Cd Y and (*b*) CdS Y.

Figures 3(*a*) and 3(*b*) show the radial distribution functions $|F(r)|$ around the Cd atom for Cd Y and CdS Y, respectively. The $|F(r)|$ were obtained by Fourier transform of k multiplied by $\chi(k)$ [13]:

$$F(r) = \frac{1}{\sqrt{2\pi}} \int_{k_{min}}^{k_{max}} w(k) k \chi(k) \exp(2ikr)\, dk. \tag{1}$$

We used a Hanning window $w(k)$ to reduce the spurious peaks due to a finite integral region.

There exist two peaks at around $r = 1.8$ Å and 3.0 Å for Cd Y. For CdS Y, the two peaks seen in Cd Y disappear and a new peak appears at around $r = 2.0$ Å. This change suggests that the neighbours around the Cd atom were substantially changed after reaction with the H_2S gas.

In order to obtain the structural parameters around the Cd atom, a standard curve-fitting analysis was carried out. We have fitted Fourier-filtered $k^3\chi(k)$ by

means of the least-squares method with the following EXAFS formula based on a single-scattering approximation [13]:

$$k^3\chi(k) = S\sum_j N_j B_j(k_j)k^2 \exp(-2\sigma_j^2 k_j^2)\frac{\sin[2k_j r_j - \phi_j(k_j)]}{r_j^2}. \quad (2)$$

The weighting factor k^3 was introduced to compensate for reduction in the $\chi(k)$ amplitude in the high-k region. The subscript j specifies the neighbouring atom. $B_j(k)$ is the backward-scattering amplitude from atom j and $\phi_j(k)$ is the phase shift experienced by the photoelectron which is emitted from the central Cd atom and scattered by the neighbouring atom j. The numerical values of $B_j(k)$ and $\phi_j(k)$ are adopted from the supplementary table calculated by McKale *et al* [14]. The scaling factor S, the ratio of the experimental value to the calculated value, was selected to be 0.4. This gives 4 as the coordination number of Cd–S bonds in crystalline CdS. N_j represents the coordination number of atoms j which are situated at an average distance of r_j with the mean square displacement of σ_j^2. In this analysis, the error in the coordination number is estimated to be about 20%.

Recently Herron *et al* [3] discussed the local environments around Cd embedded in the Y zeolite pores using x-ray diffraction and EXAFS measurements. According to their results the Cd cations in Cd Y are located at the so-called SI′ sites in the sodalite cages as denoted in figure 4, where each Cd cation is coordinated to the oxygen (OZ) of the zeolite six-ring window. Additional neighbours of the Cd cation are O atoms occupying II′ and III sites in figure 4, which may be supplied by the residual water in the zeolite or by oxygen treatment during the sample preparation. Some fraction of the neighbours are Cd cations (Cd–Cd bonds, about 3.3 Å). The presence of Cd neighbours is associated with the formation of $(CdO)_4$ cubes stabilized with O atoms in the sodalite framework and with extra O atoms at the SII′ site. A significant fraction of the second shell was assigned to Cd–(Si, Al) bonds. The results of Herron *et al* for the bond distances, coordination numbers and Debye–Waller factors of Cd Y are listed in table 1.

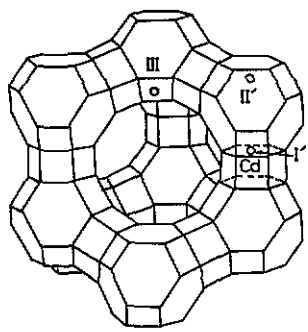

Figure 4. Some cation sites of Y zeolite, namely SI′, SII′ and SIII, are shown on the framework of (Si, Al)O_2. The vertexes represent Si or Al atoms and the full lines show (Si, Al)–O–(Si, Al) bonds. The small truncated octahedra are the sodalite cages and the large pore is the supercage.

Our data analysis on the local environment of Cd for Cd Y at 80 K was carried out by adopting the model of Herron *et al* mentioned above. It was assumed that the Cd cations reside at SI′ sites inside the smaller sodalite cages rather than inside the larger supercages. Figure 5(*a*) shows the comparison of the calculated fit of $k^3\chi(k)$ (full curve) with the Fourier-filtered spectrum (broken curve) for Cd Y. The Cd–O

Table 1. The bond distances, coordination numbers and Debye–Waller factors of Cd Y and CdS Y around a Cd atom obtained by a curve fitting of EXAFS oscillation. The structure parameters of Cd Y and CdS Y derived by Herron *et al* [3] and of crystalline CdS listed in Wyckoff [15] are also shown.

Sample	Bond	Coordination number	Bond distance (Å)	Debye–Waller factor (Å)
Cd Y	Cd–O	6.7	2.35	0.11
	Cd–O	0.6	2.61	0.014
	Cd–(Si, Al)	6.9	3.41	0.069
Cd Y	Cd–O	5.0	2.30	0.099
	Cd–(Si Al)	7.5	3.41	0.073
CdS Y	Cd–S	3.7	2.49	0.075
	Cd–O	0.3	2.28	0.031
	Cd–(Si, Al)	0.1	3.36	0.028
Cd Y [3]	Cd–OZ	3.0	2.44	0.063
	Cd–O(SII′)	2.4	2.25	0.026
	Cd–O(SIII)	2.5	2.34	0.045
	Cd–Cd	2.0	3.29	0.055
	Cd–(Si, Al)	12.4	3.42	0.037
CdS Y [3]	Cd–OZ	2.3	2.33	0.063
	Cd–O(SII′)	2.4	2.44	0.030
	Cd–O(SIII)	1.9	2.32	0.063
	Cd–S	—	2.52	0.032
	Cd–(Si, Al, Cd)	8.9	3.40	0.030
c-CdS [15]	Cd–S	4	2.52	—

bond length obtained is 2.35 Å with a coordination number of 6.7. Another oxygen neighbour is at 2.61 Å. However, the coordination number is given as 0.58, which implies the presence of a very small fraction of the additional neighbours in Cd Y. Finally, the fitting which takes account of only one kind of Cd–O bond gives 2.30 Å for the Cd–O bond length as listed in the fourth column in table 1. A reasonable fit on the second shell was obtained when the second shell was assigned to Cd–(Si, Al) bonds, i.e. the Cd cations in Cd Y are located at SI′ sites and bond to about six Si or Al atoms in the six-ring.

In contrast with the results of Herron *et al* [3], our $|F(r)|$ curve substantially changed when the Cd Y specimen was exposed to H_2S gas at 100 °C as seen in figure 3. It should be noted that the sample used in this study has nearly the same fraction of Cd cations as that used by Herron *et al*. A new peak which appears at around 1.9 Å suggests the formation of bonds between Cd and S atoms by the reaction $Cd^{2+}\text{–zeol}^{2-} + H_2S \rightleftarrows CdS + 2H^+ + \text{zeol}^{2-}$ [3]. The back Fourier transform of $F(r)$ in the region from 1.2 to 3.9 Å is shown by the broken curve in figure 5(*b*). We have fitted the filtered $k^3\chi(k)$ using equation (2) assuming that the spectrum is composed of three different bond lengths for Cd–S, Cd–O and Cd–(Si, Al) around Cd cations.

Figure 5(*b*) shows the calculated $k^3\chi(k)$ for CdS Y, which is denoted by a full curve. The agreement between Fourier-filtered and calculated spectra is satisfactory.

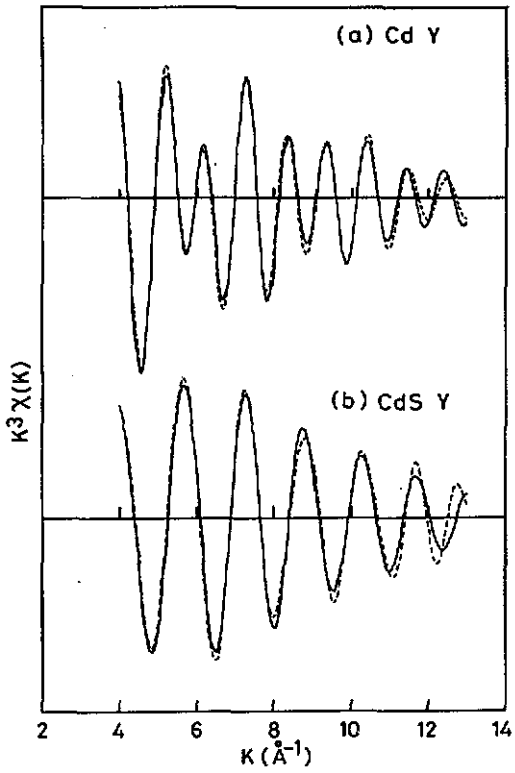

Figure 5. Comparison of the least-squares fitted spectrum (——) with the Fourier-filtered $k^3\chi(k)$ (– – –) for (*a*) Cd Y and (*b*) CdS Y.

The first shell is mainly composed of Cd–S bonds with a distance of 2.49 Å and a coordination number of 3.7. The number of Cd–O and Cd–(Si, Al) bonds is very small compared with the Cd–S bond, as seen in table 1. These results suggest that the Cd cations move out from the SI′ sites when the Cd Y specimen is exposed to H_2S gas. Since the bond distance and coordination number of Cd–S bonds in CdS Y are nearly the same as those of crystalline CdS, $(CdS)_n$ microclusters may be formed in supercages of zeolite. The average n is estimated to be about 5. The Cd and S atoms may be tetrahedrally coordinated and form a network structure, similar to crystalline CdS.

Herron *et al* [3] proposed that the addition of H_2S to Cd-exchanged zeolite does not displace Cd from the zeolite cation position and that S atoms are incorporated in $(CdO)_4$ cubes. Their conclusion is that the formation of bulk CdS could be ruled out at low CdS loading levels. We suppose that the discrepancy in the EXAFS results for CdS Y is caused by the difference between the starting zeolite species and the monitoring of the sample preparation. In the process of Cd Y production, Herron *et al* dried and calcined zeolite powder at 100 °C in flowing oxygen; consequently dehydrated zeolite may have a large amount of extra-framework O atoms. These O atoms may form a large number of $(CdO)_4$ or $(CdO, S)_4$ units.

3.2. Room-temperature absorption spectra

In figure 6 we show PA spectra obtained at about 300 K for CdS Y and CdS M samples with different Cd loadings. The full and long-dashed curves represent the PA spectra of CdS Y with 18 wt% CdS and 5 wt% CdS loadings, respectively, and

the short-dashed and chain curves represent the PA spectra of CdS M with 9 wt% CdS and 4 wt% CdS, respectively. Figure 6 also includes the spectrum of powdered crystalline CdS for comparison. The spectra are normalized by the saturated values. The shifts in the absorption edges to high energies (blue shifts) are fairly large and as much as 1 eV in CdS-encapsulated zeolites. For a given zeolite, samples show blue shifts in the absorption edges with reduction in CdS loading. This is consistent with the quantum size effect [1]. We cannot, however, define unambiguously the precise position of the absorption edges in CdS-loaded zeolites. The transition from low to high absorption is not as sharp as in a pure CdS sample. In fact, for CdS in mordenite, we find the transition region to be wider. We suspect that the size of the transition region is related to the spread in semiconductor cluster size. It appears reasonable to suppose a greater spread in cluster sizes in mordenite than in Y zeolite.

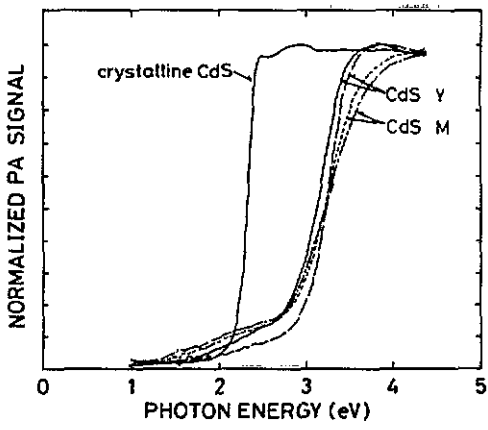

Figure 6. The PA spectra at room temperature for CdS Y (——, 18 wt% CdS; — —, 5 wt% CdS), CdS M (– – –, 9 wt% CdS; — · —, 4 wt% CdS) and powdered samples of crystalline CdS.

3.3. Photo-induced changes

PD and PB have been observed in CdS encapsulated in zeolites by illumination at low temperatures. PD refers to the metastable shift in absorption edge to a lower energy due to illumination by light with an energy greater than the band-gap energy. This can also be defined as an increase in absorption at fixed photon energies due to light exposure on a sample. In PB, a sample in a photodarkened state is illuminated at photon energies below the band-gap energy and the absorption in the vicinity of the illuminating energy decreases.

In figures 7 and 8 we show the variation in PA spectra at 70 K with increasing illumination time for CdS Y and CdS M, respectively. The energy of the illuminating light was 4.1 eV. The illumination times are indicated in the figures. The apparent shifts in absorption edges are fairly large in CdS zeolites, reaching at least 1 eV in CdS Y zeolites. Similar to the results for the PD of Se in mordenite [7], we observe at least three peaks at around 2.3, 2.9 and 3.4 eV in CdS zeolites. This is shown more clearly in figure 9 where we have plotted the difference between the illuminated and unilluminated PA spectra for CdS Y. It should be noted that the difference spectra in the high-energy region may be affected by the saturation in the PA signal. The peaks have been suggested to represent the growth of new absorption bands associated with the creation of defect states [7].

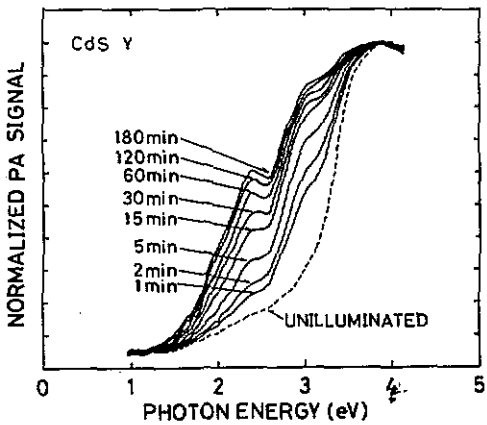

Figure 7. The PA signals of CdS Y observed after illumination with 4.13 eV light at 30 K, where the illumination times are indicated in the figure: – – –, PA spectrum of an unilluminated sample.

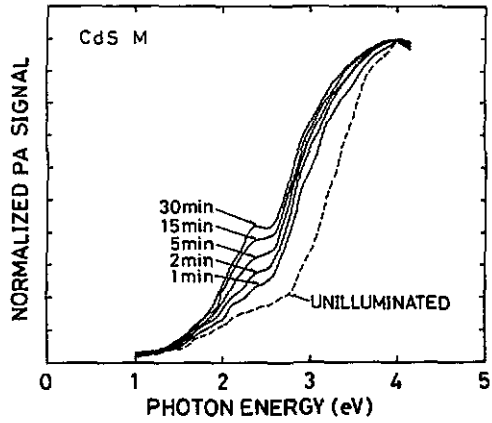

Figure 8. The PA signals of CdS M observed after illumination with 4.13 eV light at 30 K, where the illumination times are indicated in the figure: – – –, PA spectrum of an unilluminated sample.

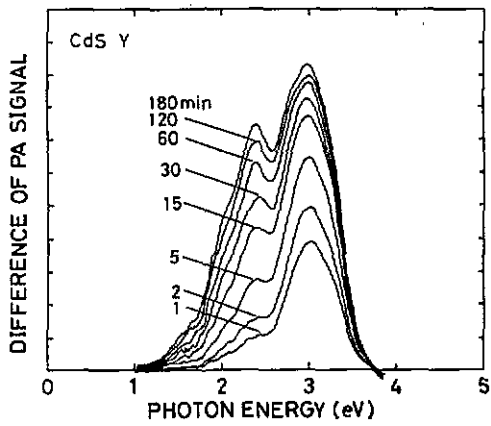

Figure 9. The differences between the PA signals of illuminated and unilluminated CdS Y where the illumination times with 4.13 eV light are indicated in the figure.

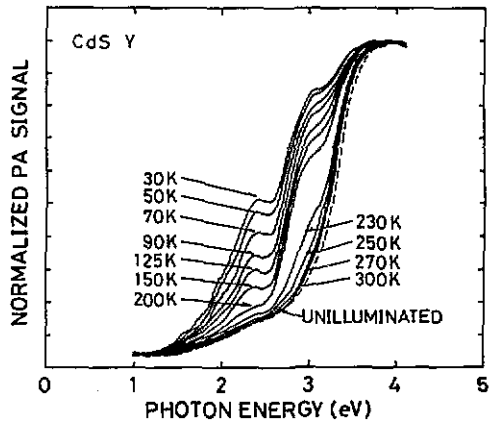

Figure 10. Annealing effect on photo-induced absorption of CdS Y where the sample was initially illuminated at 4.13 eV for 30 min at 30 K and the annealing temperatures are indicated in the figure: – – –, PA signal of unilluminated CdS Y.

From the temperature dependence of the PA spectrum we can deduce how the defect states vary with temperature. One CdS Y zeolite sample was investigated at 30 K to check the effect of temperature on the PD. Figure 10 shows the effect of annealing at various temperatures on CdS Y. The sample was initially illuminated at a photon energy of 4.13 eV for 30 min at 30 K; then the sample was warmed to the desired temperature and immediately cooled to 30 K for measurement. The results show gradual depletion of absorption peaks (figure 11) with increasing temperature. It is noticeable that the peak at around 2.9 eV is less easily annealed than that at around 2.3 eV, and the peak at around 3.4 eV remains even after annealing at 300 K. This is basically thermal bleaching with the number of defect states declining. A

more tedious way to investigate the temperature dependence of PD is to carry out illuminations at various temperatures and to cool the sample to a low temperature for measurement. Between each measurement the sample ought to be fully annealed for at least an hour at room temperature. We find similar results using these two methods. An interesting feature of the results in figures 10 and 11 is that thermal bleaching appears to slow down at high temperatures. This suggests that sufficient time has to be provided in order to annihilate thermally the defect states, even at room temperature. The PD results show that a minimum illumination energy exists below which PD is not observed. This is about 3 eV for CdS zeolites.

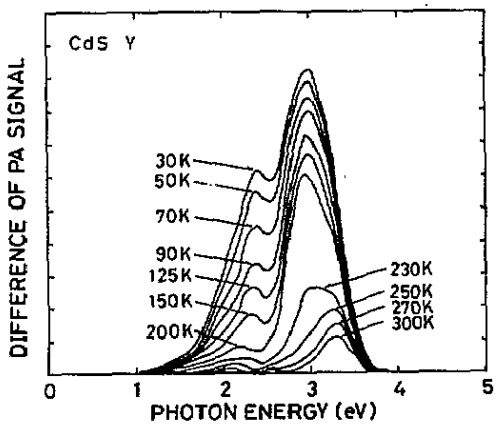

Figure 11. Annealing effect on photo-induced absorption for CdS Y. The differences between the PA signals of the illuminated and unilluminated samples are shown as a function of annealing temperature.

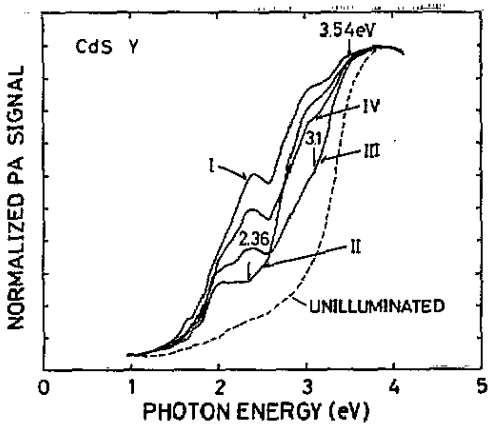

Figure 12. PB effect on CdS Y. The sample was initially illuminated with 4.13 eV light for 180 min at 30 K (curve I). Then the sample was illuminated with 2.36 eV light (curve II), 3.1 eV light (curve III) and 3.54 eV light (curve IV) in sequence. The arrows indicate the illumination energies. The PA spectrum for unilluminated CdS Y is also shown (– – –).

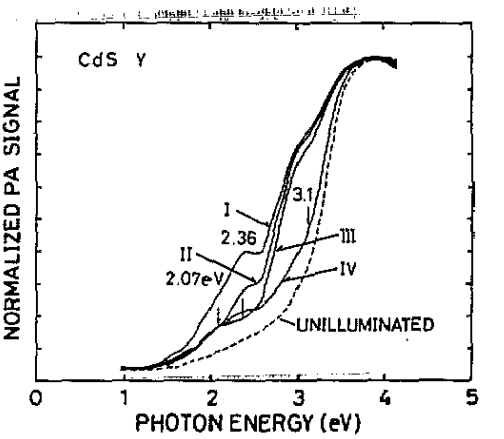

Figure 13. PB effect on CdS Y. The sample was initially illuminated with 3.81 eV light for 30 min at 30 K (curve I). Then the sample was illuminated with 2.07 eV light (curve II), 2.36 eV light (curve III) and 3.1 eV light (curve IV) in sequence. The arrows indicate illumination energies. The PA spectrum for unilluminated CdS Y is also shown (– – –).

The results of PB by illumination with photon energies below the absorption edges are displayed in figures 12 and 13 for CdS zeolite. Initially the samples were photodarkened by above-band-gap light at 30 K. The illuminating photon energies during bleaching were selected at the peak positions of the photo-induced absorption bands created during PD. The PB tended to saturate rather quickly after illuminations of at least 10 min. In figure 12 we show the PB effect in CdS Y. The sample was initially illuminated with 4.13 eV light for 180 min at 30 K (curve I). Then the sample was illuminated with 2.36 eV light (curve II), 3.10 eV light (curve III) and 3.54 eV light (curve IV) in sequence. The broken curve represents the PA spectrum of an unilluminated CdS Y sample. We observe suppression of absorption in the vicinity of the illuminating energy. States in the vicinity of 2 eV appear not to become bleached. PB at a higher energy causes some PD at a lower energy. However, if we start bleaching from 2.07 eV, we find a more or less systematic decrease in the number of defect states (figure 13). The sample was initially illuminated with 3.81 eV light for 30 min at 30 K (curve I). Then the sample was illuminated with 2.07 eV light (curve II), 2.36 eV light (curve III) and 3.10 eV light (curve IV) in sequence. Slight asymmetry on the left shoulder of the peak at around 2.3 eV appears to indicate another peak or an extra absorption band in the vicinity of 2 eV. Hence four new absorption bands appear to be created by illumination in CdS zeolites.

PB can be explained as a consequence of the annihilation of defect states [7, 16] through excitations by photons. We note that in a photodarkened state a defect can relax to an unphotodarkened state by thermal relaxation. The probability of this is quite small at low temperatures but, when excited, a defect has a higher probability of relaxing to an unphotodarkened state.

Defect creation during illumination has been suggested to be the result of the weakening or breaking of bonds [6]. The nature of bonding in CdS microclusters inside zeolites is not entirely obvious and the actual form of the clusters is still not clear. Better insight into cluster formation can probably be obtained by monitoring the sample preparation more systematically. Our preliminary PD results on a Cd Y sample which had been exposed to H_2S at room temperature are shown in figure 14 by the broken curve. It shows a reduction in PD and a shift in absorption edges to a higher energy with respect to a sample heated at 100 °C (dotted curve). The differences in PD were also obtained for two samples with the same Cd loading but annealed at 100 °C and 150 °C, respectively.

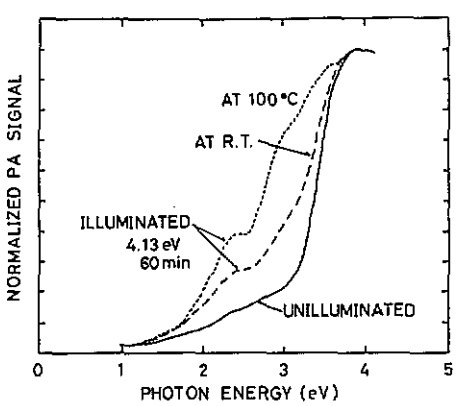

Figure 14. Comparison of the PD effect on CdS Y samples with different annealing procedures: – – –, sample exposed to H_2S gas at room temperature (RT) and not heated; ·····, sample heated at 100 °C for 1 d; ——, PA spectrum for an unilluminated CdS Y sample.

4. Conclusions

CdS microclusters grown in zeolite pores have been found to exhibit PD. The amount of PD depends critically on the reaction temperature, the measurement temperature, the photon energy and intensity, and the Cd loading of the samples. It is not possible to say that this is a genuine effect of changing the chalcogen atom. This is because the techniques used to produce the samples are different and PD is rather sensitive to the annealing temperature.

Although we can explain PD as a consequence of the creation and annihilation of defect states [6], it is important to know the nature and origin of defects and how they affect observed results. In CdS zeolites we have found indications for four new absorption bands induced by illumination during PD. Although many models such as the two-polaron model [17] are proposed to understand the PD and PB effects, the mechanism for the photo-induced phenomena of CdS Y is still not clear.

The nature of CdS clusters in zeolites does not seem to be fully resolved. The sensitivity of the optical spectra to the annealing temperature suggests that CdS molecules or clusters can migrate and form larger clusters or more extended chains or rings within zeolite pores. Hence it is unlikely that the Cd arrangement stays unchanged upon reaction with H_2S in our samples. This is consistent with the EXAFS results. We suspect that larger clusters can also easily form within the supercages.

Acknowledgment

One of us (TM) is indebted to the Matsumae International Foundation for financial support while in Japan.

References

[1] Ekimov A I, Efros Al L and Onushchenko A A 1985 *Solid State Commun.* **56** 921
[2] Wang Y and Herron N 1987 *J. Phys. Chem.* **91** 257
[3] Herron N, Wang Y, Eddy M M, Stucky G D, Cox D E, Moller K and Bein T 1989 *J. Am. Chem. Soc.* **111** 530
[4] Moller K, Eddy M M, Stucky G D, Herron N and Bein T 1989 *J. Am. Chem. Soc.* **111** 2564
[5] Tang Z K, Nozue Y and Goto T 1991 *J. Phys. Soc. Japan* **60** 2090
[6] Elliot S R 1986 *J. Non-Cryst. Solids* **81** 71
[7] Katayama Y, Yao M, Ajiro Y, Inui M and Endo H 1989 *J. Phys. Soc. Japan* **58** 1811
[8] Katayama Y, Maruyama K, Yao M and Endo H 1991 *J. Phys. Soc. Japan* **60** 2229
[9] Katayama Y, Maruyama K and Endo H 1990 *J. Non-Cryst. Solids* **117–8** 485
[10] Beck D W 1974 *Zeolite Molecular Sieves* (New York: Wiley)
[11] Nomura M and Koyama A 1989 *KEK Report* **89-16**
[12] Inui M, Yao M and Endo H 1988 *J. Phys. Soc. Japan* **57** 553
[13] Teo B-K 1986 *EXAFS: Basic Principles and Data Analysis* (Berlin: Springer)
[14] McKale A G, Veal B W, Paulikas A P, Chan S-K and Knapp G S 1988 *J. Am. Chem. Soc.* **111** 3763
[15] Wyckoff R W G 1963 *Crystal Structures* vol 1, 2nd edn (New York: Wiley) ch III
[16] Ducharme S, Hautala J and Taylor P C 1990 *Phys. Rev.* B **41** 12250
[17] Ikawa A and Fukutome H 1990 *J. Phys. Soc. Japan* **59** 1002